



ELSEVIER

Contents lists available at SciVerse ScienceDirect

## Computers &amp; Geosciences

journal homepage: [www.elsevier.com/locate/cageo](http://www.elsevier.com/locate/cageo)

# CHRISTINE code for High resolution satellite mapping of optical thickness and Ångström exponent, Part II: First application to the urban area of Athens—Greece and comparison to results from previous contrast-reduction codes

Nicolas I. Sifakis<sup>a,\*</sup>, Christos Iossifidis<sup>b</sup>, Charis Kontoes<sup>c</sup><sup>a</sup> Institute for Space Applications and Remote Sensing, National Observatory of Athens, currently seconded to the European Research Council Executive Agency, Brussels, Belgium<sup>b</sup> School of Rural and Land Surveying Engineers, National Technical University of Athens, Heroon Polytechniou 9, GR-15780 Zografou, Greece<sup>c</sup> Institute for Space Applications and Remote Sensing, National Observatory of Athens, Metaxa and Vassileos Pavlou, GR-15236 Pendeli, Greece

## ARTICLE INFO

## Article history:

Received 14 June 2012

Received in revised form

22 April 2013

Accepted 15 May 2013

## Keywords:

High resolution

Air pollution

Urban

Aerosol optical thickness

Ångström

## ABSTRACT

There is an increasing demand for exploiting satellite data in urban air quality assessment. High spatial resolution satellite data can be used to retrieve the aerosol optical thickness (AOT), as an air quality indicator, over urban areas. One of the methods to achieve this applies the contrast-reduction principle to a set of two satellite images, one of which has minimum aerosol content and is used as a reference. Previous satellite image processing codes that followed this approach were subject to surface changes which may have occurred in the time interval between the processed images acquisition. In order to eliminate this potential source of AOT miscalculation the CHRISTINE Code for High Resolution Satellite Mapping of Optical Thickness and Ångström Exponent was developed. This new code takes into consideration contrast reduction in more than one spectral band, and applies the Ångström's law to isolate atmospheric and surface components. The code underwent its first testing using Landsat satellite data acquired before 2001 (when air pollution was at its peak) over the study area of Athens (Greece). Results showed that CHRISTINE can effectively separate contrast modifications attributed to atmospheric changes from those due to surface changes. Comparison against the previous SMA Satellite Mapping of Aerosols code showed an average improvement of 21% in terms of area over which AOT could be retrieved with high confidence. CHRISTINE also approximates the aerosol size distribution over the studied area. These preliminary findings show that the new code can be used to counteract for spatial deficiencies in urban monitoring networks. In the case of Athens the application to archived satellite data also allowed hindcasts for the period prior to ground based aerosol measurements.

© 2013 Elsevier Ltd. All rights reserved.

## 1. Introduction

Urban air-quality measurements are heavily based on in-situ measurements of pollutants by ground based stations, which lack spatial continuity and may not be readily available in remote areas and developing countries (Gupta et al., 2006). This leads to an increasing demand for exploitation of satellite data. Unfortunately, while satellite remote sensing has become a valuable tool for assessing atmospheric pollutants at a global level (Borowiak and Dentener, 2006), there has been little effort to map air quality at detailed level, namely at the urban scale (Nichol and Wong, 2009). A poor collaboration between air pollution and remote sensing

scientists as well as limited resources (both financially and in trained personnel) of the urban air quality monitoring sector are at the origin of this deficiency (Engel-Cox et al., 2004). Another reason for this is that no satellite mission aims at monitoring urban air pollution with fine spatial resolution.

A few satellite sensors, such as TOMS and GOME, and more recently MOPITT, AIRS and SCIAMACHY, gather systematically data on atmospheric species including aerosols and selected gases. The low spatial resolution (i.e., tens of kilometers) of these spectrometers is relevant to the spatial domain of global scale studies. On the other hand, optical satellite sensors estimate the aerosol load in terms of columnar aerosol optical thickness (AOT) which, when divided by the atmospheric mixing height (Dandou et al., 2002), can be converted to scattering coefficient values ( $k_{\text{scat}}$ ) predicting particle concentrations at ground level (Jiang et al., 2007; Liu et al., 2007) particularly PM<sub>2.5</sub> mainly during

\* Corresponding author. Tel.: +30 210 810 9187; fax: +30 210 613 8343.  
E-mail address: [sifakis@noa.gr](mailto:sifakis@noa.gr) (N.I. Sifakis).

winter conditions (Schaefer et al., 2008). AOT may be retrieved at various spatial resolutions by assessing the influence of the aerosols to satellite radiometry. More specifically, the polar AVHRR and ATSR-2, and the geostationary GOES-8 and SEVIRI may retrieve AOT with moderate spatial resolution (i.e., few kilometers), but they address large scale pollution phenomena (e.g., Popp et al., 2007). MODIS and MERIS provide on a daily basis standardized products on aerosol load and properties at moderate-to-high spatial resolution (i.e., hundred meters) and they can cover regional scale phenomena (e.g., Chu et al., 2003; Von Hoyningen-Huene et al., 2003; Tang et al., 2005; Liang et al., 2006; Kokhanovsky et al., 2007). The last generation of very high spatial resolution sensors (ground sampling distances of less than a meter), such as IKONOS-2, Quickbird, GeoEye-1 and WorldView-1, may provide circumstantial information on air pollution (e.g., visible pollution plumes) or on ancillary parameters influencing emissions and dispersion (e.g., land cover, traffic load, terrain roughness) (Eikvil et al., 2009). Finally, the latest active satellite lidar instruments, such as CALIPSO, allow to accurately assessing aerosol properties and load, but they focus on the vertical not the horizontal distribution.

The current study focuses on the use of high spatial resolution (HSR) sensors (i.e., resolution from tens to a few hundreds of meters), such as Landsat TM/ETM+, SPOT HRV/HRVIR and IRS LISS-III, that pre-date most of the optical sensors previously mentioned but address land and sea rather than atmospheric observations. Nonetheless, qualitative atmospheric observations using HSR sensors were cited as early as in the 70s; they concerned smoke emitted from industrial/urban sites or from forest fires (Short et al., 1976), assessment of pollution associated to statistical indicators (Potter and Medlowitz, 1975) and aerosol estimations over water (Griggs, 1975). The first quantitative pollution assessments appeared in the early 80s (Fraser et al., 1984), and attempts for pollution mapping started in the late 80s (Sifakis, 1987; Tanré et al., 1988) and early 90s (Sifakis and Deschamps, 1992). The use of HSR satellites to map over urban areas progressively received further attention from various researchers who have developed a range of techniques with respective limitations (e.g., Kocifaj and Horvath, 2005). For example, the “clear water” method can be used only above water surfaces (Gordon and Clark, 1981) while the dense dark vegetation (DDV) method, requires the presence of vegetated areas (Kaufman and Sendra, 1988), and the “deep blue” method, proposed by Hsu et al. (2004), has shown satisfactory results over bright targets but is applicable only to satellite sensors with bands sensitive in the blue spectral area. Finally, the “contrast-reduction” principle, namely the apparent or observed-at-satellite reduction of contrast between distinct surface targets, engendered by the scattering mechanism of aerosols in the visible and infrared spectral areas, gives satisfactory results over urban areas, composed by heterogeneous land parcels. This part of the study (Part II) aims at applying the new Code for High Resolution Satellite Mapping of Optical Thickness and Ångström Exponent (CHRISTINE), developed in Part I of this article, to HSR data of the Athens urban area and for the years prior to 2001 when no ground measurement on aerosol concentrations was yet available.

The CHRISTINE code applies the contrast reduction principle to a set of two satellite images, one of which has minimum aerosol content and is used as a reference. Contrast reduction was first described by Middleton (1952) through the Koschmieder's equation:

$$C/C_0 = \exp(-AOT) \quad (1)$$

where  $C$  is the observed and  $C_0$  the real contrast of a target. Eq. (1) gives an idea of the sensitive dependence of AOT on contrast reduction. Contrast reduction may also be sensitive to other than atmospheric variations; previous contrast reduction codes were subject to surface changes which may have occurred in the time

interval between the processed images acquisition. In order to eliminate this potential source of AOT miscalculation CHRISTINE takes into consideration contrast reduction in more than one spectral band, allowing to separate contrast modifications attributed to atmospheric changes from those due to surface changes. This increases the area over which AOT can be retrieved with higher level of confidence. The new code furthermore provides an approximation of the Ångström coefficient and creates maps depicting the aerosol size distribution.

## 2. Methodology

### 2.1. Study area

The geographic area selected for testing the new code covers the Greater Athens Area (i.e., the Athens basin). This region is well known for air pollution problems and the prior existence of a large body of associated studies (e.g., Kambezidis et al., 1998). Athens is a city with a history of environmental, particularly air quality, problems (Kambezidis and Sifakis, 2004). It accommodates a population of about 3.5 million inhabitants (census 2001). Most of the population live within the Athens basin, which is an elongated bowl oriented along a NE–SW axis with mountains on all sides (ranging from 400 to 1200 m a.m.s.l.), and the sea to the south (Saronikos Gulf) (Fig. 1). Predominant winds flow around the year in the NE–SW direction but because of the orographic setting air pollution is often confined in the basin. The climate in Athens is Mediterranean with mild winters (mean seasonal air temperature of 9.9 °C), warm summers (mean seasonal air temperature of 25.8 °C) and annual rainfall of about 418 mm. Solar radiation is rather strong with average diurnal values (on a horizontal surface) of the order of 22 MJ m<sup>-2</sup> in the summer and 8 MJ m<sup>-2</sup> in the winter. Sea-breeze cells develop along the main NE–SW axis of the basin in late spring and the summer while during summer northerly strong (Etesian winds) usually blow. Apart from the traffic, some industrial activities exist in the western part of the Athens basin. Due to working hours there is a peak in air pollution at around 8h00 LST (Kambezidis et al., 1995). Since 1984 the Division of Air Quality and Noise Control (EARTH) of the Ministry of Environment, Physical Planning and Public Works is responsible for air quality monitoring in the Athens area. A number of studies have been devoted to the air pollution problem in Athens aiming at analyzing the conditions favouring air pollution episodes, via computer simulations (e.g., Cvitaš et al., 1985) and at experimental level (e.g., Scheff and Valiozis, 1990).

### 2.2. Landsat satellite data

The satellite data used to test the new code were Landsat 5 and Landsat 7 high spatial resolution images covering the Athens basin. A large portion of the image data sets were acquired in the framework of a project concerned with “Retrospective Mapping of Air Pollution in Athens by Satellite” for the years prior to 2001, in particular between 1986 and 2001, when no ground measurement on aerosol concentrations (in terms of PM10) was yet available. Therefore the selection of the satellite images was based on: (i) on the availability of HSR satellite data acquired in that time period over the study area, (ii) the pollution level data from the local ground based stations. Only high quality images acquired under extremely low cloud cover were considered as candidates. Since no aerosol concentration data were available before 2001, pollution levels for the respective acquisition dates were assessed on the basis of data on gaseous pollutants from the EARTH monitoring network. More specifically the average concentration between all available stations for two basic pollutants,

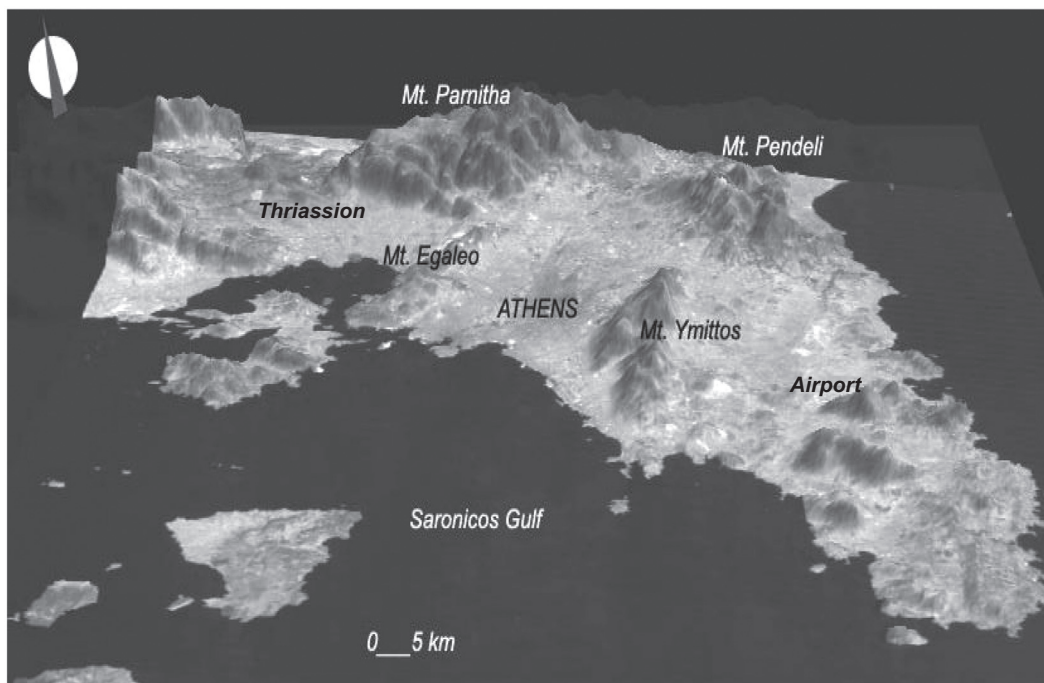


Fig. 1. 3D view of the Greater Athens Area derived by a combination of a Landsat image and a digital elevation model.

Table 1

Landsat satellite images selected over the Athens study area.

Date	Satellite	Ranking for respective year
1 25 July 1986	Landsat 5	7th most polluted
2 10 June 1987	Landsat 5	5th most polluted
3 31 August 1988	Landsat 5	3rd most polluted
4 23 February 1989	Landsat 5	18th most polluted
5 21 June 1991	Landsat 5	19th most polluted
6 16 October 1993	Landsat 5	16th most polluted
7 26 April 1994	Landsat 5	19th most polluted
8 31 May 1995	Landsat 5	15th most polluted
9 4 July 1996	Landsat 5	3rd most polluted
10 20 May 1997	Landsat 5	3rd most polluted
11 24 June 1998	Landsat 5	10th most polluted
12 8 April 1999	Landsat 5	18th most polluted
13 5 June 2000	Landsat 5	Landsat 5 reference (225th most polluted)
14 16 August 2000	Landsat 7	Landsat 7 reference (237th most polluted)
15 26 July 2001	Landsat 5	4th most polluted

NO<sub>2</sub> and SO<sub>2</sub>, was calculated for each satellite acquisition date. The ratio between these spatial averages and the maximum annual value for the respective year was subsequently determined. This allowed ranking each image according to the pollution levels of the respective acquisition date with respect to the most polluted day of that year. Finally the most polluted available image for each year was selected (Table 1).

Table 1 indicates that 100% of the selected “polluted” images corresponded to the 20 most polluted days of the respective years, while 50% corresponded to the 10 most polluted days of the respective years. This rendered the selected satellite images representative in terms of pollution levels. Almost all of these images were acquired in the spring and early summer period, when the highest pollution levels in Athens are usually being recorded (Lalas et al., 1983). The selection of the so-called “reference”, which is a pollution-free image, was based on the inverse procedure. Fig. 2 describes the distinct stages followed when selecting the optimal satellite images.

Fifteen Landsat images were selected in the years 1986–2001 and underwent the necessary pre-processing, including a geometrical

control (super-imposition) of all the images, and a geo-rectification according to a topographic map. For the latter the “nearest-neighbor” algorithm was used in order to avoid altering the raw radiometric values and the initial distribution pattern of the pixels. For the same reason no stretching or other contrast enhancement technique was applied to the histograms of the images. Subsequently all information referring to water-surface was removed by respective “masking”. The geo-rectification of the images, carried out during preprocessing, resulted into a geometrical accuracy of the order of half a pixel.

### 2.3. Application of the code

The CHRISTINE code was used to retrieve AOT and map its horizontal distribution from the satellite images. This code uses the contrast reduction method over an array superimposed to satellite images. In the case of Landsat imagery each array cell comprises 17 × 17 pixels, which is a compromise between an array small enough for the atmosphere to be considered homogeneous (so that AOT values are representative for any array area), and large enough for the surface to be considered heterogeneous (so that contrast values are significant). While retrieved AOT values are attributed to the central pixel of each cell, covering an area of 0.5 km by 0.5 km, the final resolution of the produced AOT maps corresponds to the sensor's spatial resolution. In comparison to previous DTA/SMA codes, CHRISTINE assesses contrast reduction in consecutive spectral bands. Theoretically six of the seven Landsat TM/ETM+ spectral bands can be used, since contrast reduction by scattering mechanism is not significant in the thermal infrared (band 6). Furthermore, information brought by bands 5 and 7 is considered redundant since AOT values are too low in the shortwave infrared for the atmospheric-signal-to-ground-noise ratio to be significant. Therefore CHRISTINE utilizes bands 1, 2, 3 and 4 in the blue, green, red and near infrared spectral areas respectively, to calculate spectral AOT by quantifying contrast reduction using Eq. (2) presented in the companion paper: “Part I: Algorithm and Code”. The spectral variability of AOT is subsequently assessed as a function of the Ångström coefficient on the basis of Eq. (1) presented in the companion paper: “Part I: Algorithm and Code”.

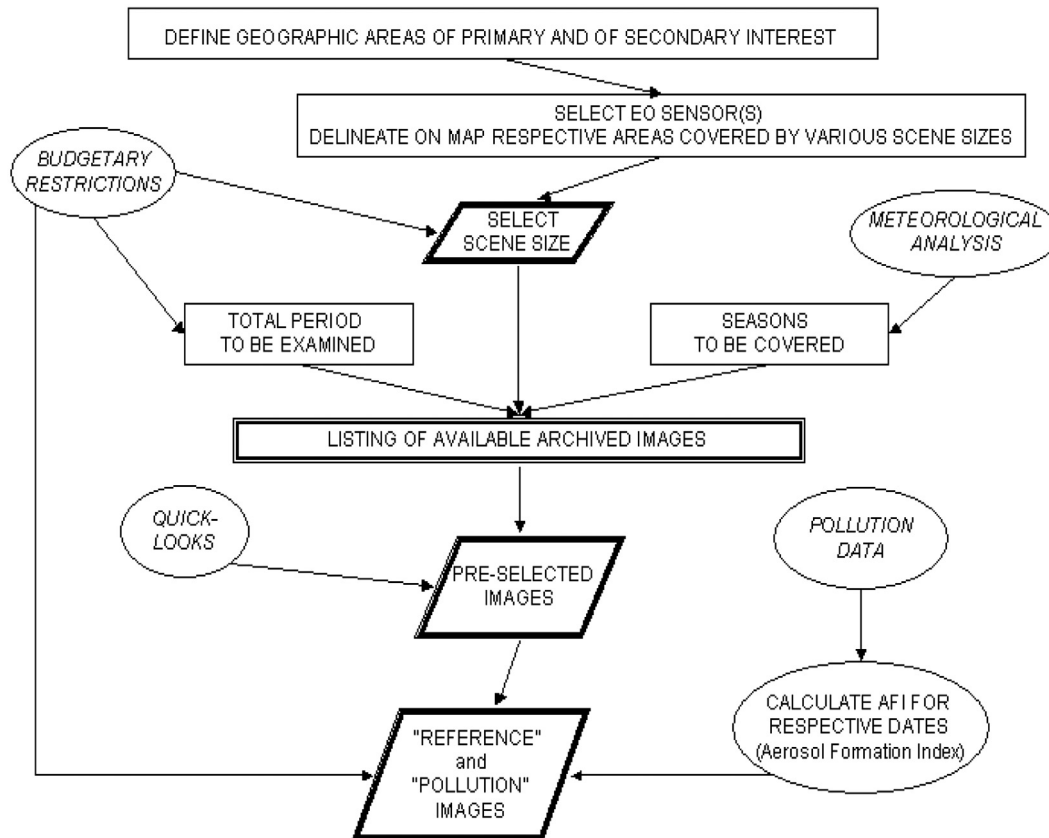


Fig. 2. Suggested procedure for the selection of optimal satellite images.

### 3. Results

The primary outcome of CHRISTINE is a map depicting the horizontal distribution of AOT. Fig. 3 depicts 12 of the 13 AOT maps resulted from the application of the code to the selected images. These maps depict the spatial distribution of urban aerosols over the Athens basin during typical pollution days between 1986 and 2001. The first thing to notice is that the pollution cloud is confined, in all but two cases inside the basin around the city center. In two acquisitions (i.e., 1986 and 1987) there bulk of the pollution is observed over the area of Thriassion, west of the basin and of Mt. Egaleo, where the main industrial activities were then concentrated. In most cases, pollution spots are also observed to the northern suburbs towards the foot of Parnitha and Pendeli mountains. This is probably transported pollution associated to the formation of a thermal internal boundary layer due to sea-breeze circulation from Saronikos Gulf or weak southerly flow conditions associated with calm conditions inside the basin (Lalas et al., 1983). It is noteworthy that it is the first time that this phenomenon is observed through high resolution satellite imagery.

Additional observations on the spatial distribution of air pollution, specific to selected dates, are drawn hereafter (right column in Fig. 4):

- The image of 26.04.1994 (first row from top in Fig. 4) captured a typical air pollution episode during springtime; high pollution levels were recorded inside the Athens basin which is clearly depicted by the AOT distribution map. Meteorological data show that an anticyclone combined to the transportation of warm air masses resulted in a limited vertical development of the mixing layer. The main pollution load is detected over the city center while the rest of pollution is confined inside the Athens basin and dispersed along the south coast.

- The image of 31.05.1995 (second row from top in Fig. 4) depicts moderate to high pollution levels detected above the city center as well as towards the north-eastern suburbs against Mt. Ymittos.
- The image of 04.07.1996 (third row from top in Fig. 4) is a summertime acquisition showing moderate pollution levels over the Athens basin. The bulk of pollution is confined inside the basin mainly along a southwest-northeast axis, which is perpendicular to the coast, due to the typical sea breeze mechanism developed in the area.
- The image of 20.05.1997 (last row from top in Fig. 4) revealed a second springtime pollution episode, similar to the first but where the intense pollution over and around the city center is also spread towards the north-eastern suburbs covering almost the entire basin.

The results of the new code were subsequently compared to those of the previous SMA code. Fig. 4 juxtaposes the results obtained by the two codes: the left column presents results by SMA while the right column presents results by CHRISTINE. When comparing the two subsets of maps depicting the spatial distribution of urban aerosols, the subset derived by the CHRISTINE code contains significantly less artifacts associated to land cover changes. In general all maps derived by the new code contain less noise and present more clearly identified boundaries between the various AOT classes. The total area covered by classified AOT over land (confident AOT retrieval) is smaller in the case of CHRISTINE. This is due to a stricter criterion used for AOT retrieval by CHRISTINE that is, AOT is retrieved over fewer areas but with higher levels of confidence. A typical observation relates to a characteristic Z-shaped area, erroneously revealing high AOT values in all SMA maps (Fig. 4 encircled in top row, 1994). This artifact is located to the east of Mt. Ymittos, outside the Athens

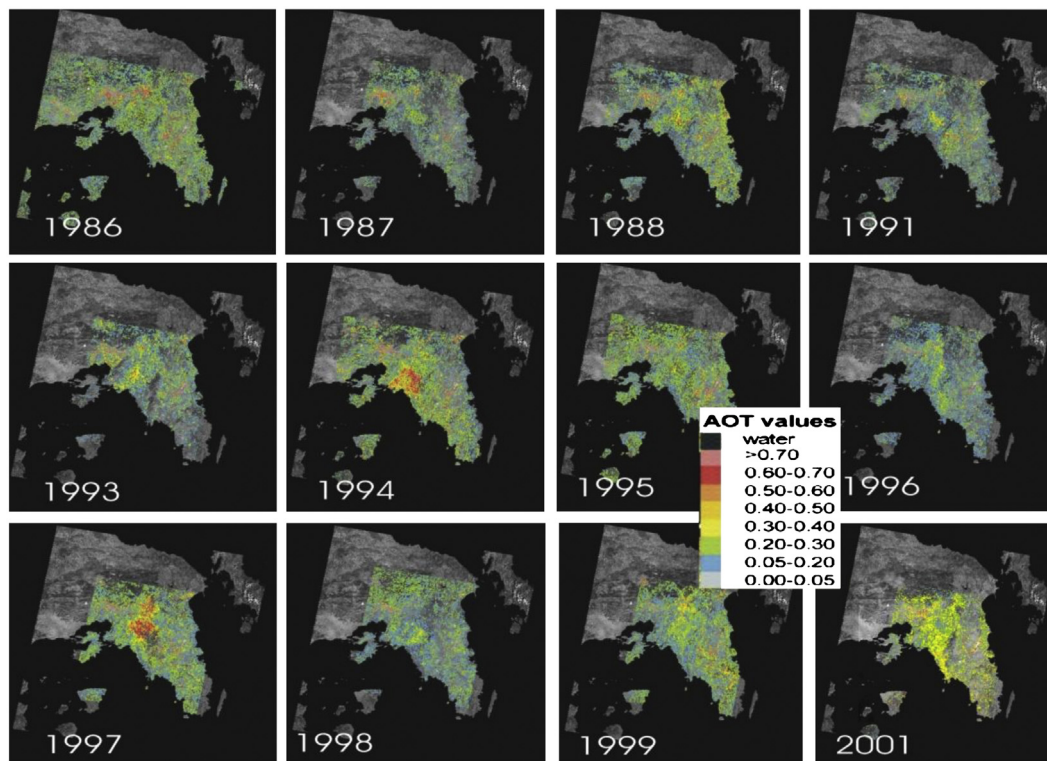


Fig. 3. AOT Landsat satellite based map series between 1986 and 2001 over Athens.

basin, where air pollution is expected to be less significant; it is attributed to extended excavations that took place at the new airport (El. Venizelos) along with part of the ring road (Attiki Odos) in the year 2000 when the reference image was acquired. The pollution images had been acquired before the excavation works (1994–1997) when the soil's surface reflectance was still homogeneous, thus less contrasted, compared to that in the reference image due to the excavations. This resulted in an apparent contrast reduction that caused an erroneous appraisal of AOT values by the SMA code. CHRISTINE has successfully isolated and eliminated this artifact and by excluding the area from AOT retrieval as non confident.

The following observations, specific to two of the examined images, allow further evaluating the performances of the new code:

1. On the AOT map of 31.05.1995 (Fig. 4, second row from top), along with the Z-shape eliminated area, few other artifacts have been masked out in the upper right part of the image (i.e., over Mt. Pendeli). These areas are probably associated with wildfires that took place during the summer of 1994.
2. On the map of 20.05.1997 (Fig. 4, bottom row) the code has masked out all artifacts described in the previous case (31.05.1995) plus a large area on Mt. Ymittos (southeast of the city center), which is associated to a wildfire that occurred in the summer of 1996.

Overly, the testing of the CHRISTINE code over Athens against results obtained using the SMA code showed an average reduction of noise of 27% in terms of area over which AOT was retrieved with high levels of confidence.

AOT values generated by the code were finally compared to pollution data. Hourly concentration values of pollutants recorded by the EARTH national monitoring network were used to this end. This network is composed by 18 stations, today monitoring most of the common gaseous and particulate air pollutant

concentrations. Since, however,  $PM_{10}$  measurements had not been carried out by this network until 2001, sulfur and nitrogen dioxide concentration levels (as gaseous precursors of ammonium sulfates and ammonium nitrates secondary aerosols) were used for the comparison with satellite based AOT values. The comparison was not a straight forward also for another reason: satellite based measurements are vertically averaged while ground based data on pollutant concentrations consist of point measurements. Nonetheless we can assumed that, since aerosol sources are on the surface, pollution particles are mainly accumulated in the troposphere and most particularly in its lowest part, generally at an altitude of less than 1.5 km of altitude (Lenoble, 1993). Fig. 5 shows a significant correlation between satellite AOT retrieval and ground based  $SO_2$  in the Athens area. The linear correlation of the two indirectly related parameters is of the order of 70%, which can be explained by the fact that ammonium sulfates are produced, in the form of optically effective secondary aerosol, when sulfur dioxide is oxidized into particles of sulfuric acid, then react with ammonia in the atmosphere (part of urea synthesis) (Colls, 1997). The optical effects of this secondary aerosol are virtually determined within the first kilometer(s) of the ground (Fraser et al., 1983). The above correlation clearly shows that  $SO_2$  can, for the examined years, explain an important part of satellite based AOT's spatial fluctuations, while another part could be explained by other optically effective atmospheric pollutants such as ammonium nitrates or soot.

Direct comparisons between ground based aerosol concentrations (PM) and AOT retrieval using the previous contrast-reduction based codes (DTA/SMA) is provided by Sarigiannis et al. (2004), who used post-2001 Landsat satellite images of the urban area of Athens. This author reported a correlation of 0.96 between AOT and particulate concentrations over the ground pollution monitoring stations in Athens. The respective correlation coefficient using MERIS moderate resolution satellite data varied from 0.63 to 0.88 for the different ground stations in Athens (Retalis and Sifakis, 2010).

The second output of the CHRISTINE code is a map depicting the spatial distribution of an approximated Ångström coefficient;

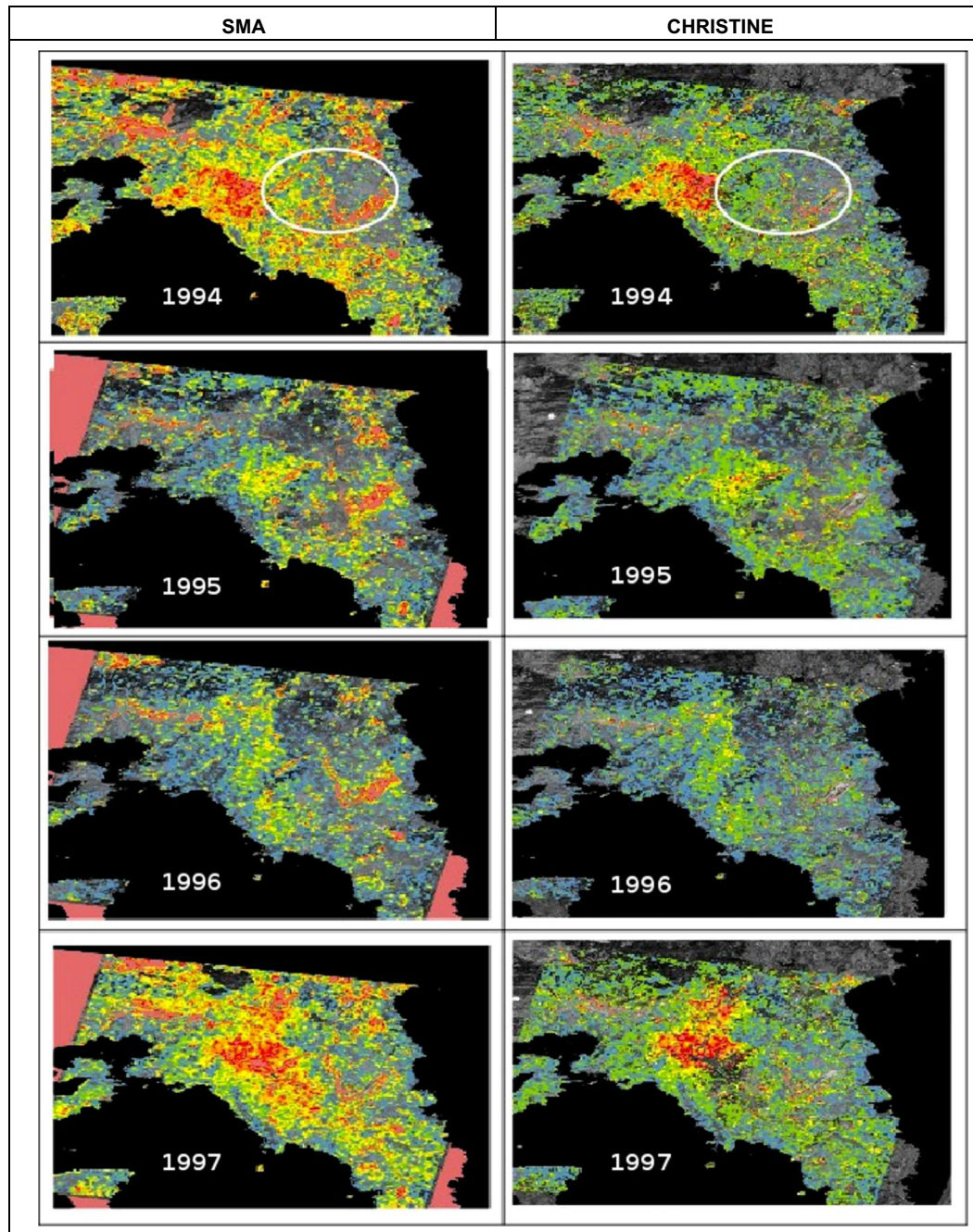


**Fig. 4.** AOT satellite maps over Athens. Dates from top to bottom: 26.04.1994, 31.05.1995, 04.07.1996, 20.05.1997. Left column images show results obtained using the SMA code while right column images depict results using the CHRISTINE code.

while some works have already compared experimental data and modeling estimates of AOT and Ångström coefficient over the Athens basin, no study has yet attempted to assess the Ångström coefficient on the basis of high resolution satellite data. According to Kaskaoutis et al. (2006a) the errors in Ångström, over the Athens area, become larger at low AOT values. Therefore the characterization of aerosols can be performed best under high aerosol burden conditions, as is the case for the 26.04.1994. Fig. 6 presents the horizontal distribution of the Ångström coefficient over the Athens area for the previous date, resulting from the application of CHRISTINE code to Landsat data.

Since no ground truth information with respect to particle size distribution was available for that date, validation was based on

qualitative interpretations based on local and collateral information. A first observation is that the Ångström exponent increases ( $\alpha > 0.5$ ) over the city center and towards the western part of the city. This may indicate that smaller particles predominate, which is reasonable as the principal anthropogenic emission sources are located in those areas. The Ångström exponent decreases ( $\alpha < 0.5$ ) toward the suburbs meaning that particles grow as they spread, by gas-to-particle conversion, coagulation and humidification processes. In this typical pollution-episode day of the 26th of April 1994 the dominant aerosol type is characterized by an Ångström exponent varying from 1.5, over the emission sources, to 0.5 further downstream; these figures are common for urban hazes including dust and sea salt aerosols (Kaskaoutis et al., 2006b; Marey et al., 2010).

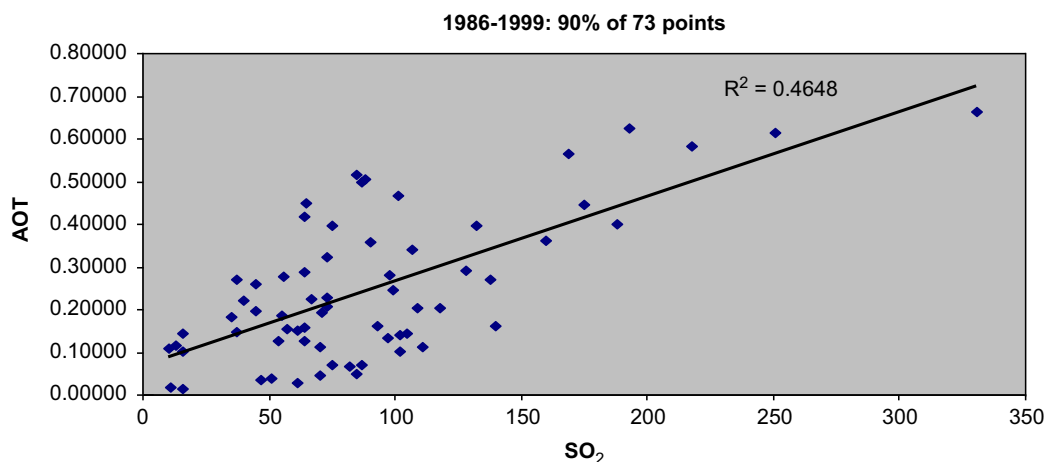


Fig. 5. Satellite derived AOT (Landsat images) vs. ground based  $\text{SO}_2$  for 90% of all common available measurements.

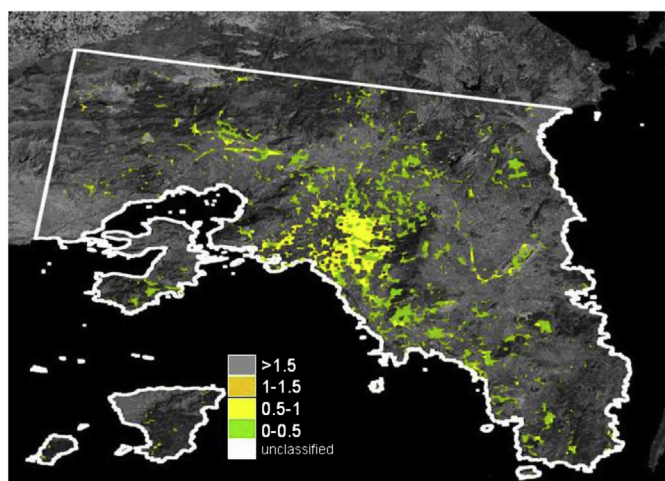


Fig. 6. Ångstrom exponent map on 26.04.1994 over Athens derived by the application of the CHRISTINE code to Landsat data.

#### 4. Summary and conclusions

A new image processing code (CHRISTINE) for high resolution satellite mapping of aerosol optical thickness (AOT) and Ångstrom coefficient approximation underwent its first testing. The code is based on the contrast reduction principle between a reference satellite image (with minimum aerosol content) and an examined image. The new code intends to overcome an important limitation of the previous (DTA and SMA) codes: their sensitivity to artifacts attributed to ground reflectance variations between the reference and the examined image. This is achieved by considering contrast reduction in consecutive spectral bands (i.e., in the visible and the near infrared) endeavoring to decouple “atmospheric signal” from “ground noise” during AOT retrieval. In an attempt to characterize the aerosol size distribution, the new code also performs an approximation of the average Ångstrom exponent.

The new code was applied to high spatial resolution Landsat TM/ETM+ data, which allowed for the production of AOT maps with a ground sampling distance of 30 m. This information on the distribution of aerosols is extremely dense in comparison to ground based monitoring networks, and can be particularly useful over complex urban terrains with street canyons, building blocks and topography that continuously modulate the diffuse and advective transport of pollutants. The code was preliminary tested over the Athens basin (Greece) well known for frequent pollution episodes. Archived

Landsat 5 TM and Landsat 7 ETM+ satellite data, coinciding with characteristic pollution conditions in the period 1986–2001, were used. Since no aerosol concentration data measurements were carried out for that period in Athens, the results from this application allowed quantifying particulate air pollution, in terms of AOT, and visualizing its spatial distribution over Athens during typical pollution conditions. The comparison with AOT results obtained by the previous SMA code yielded a clear advantage of the new code: the criteria applied by CHRISTINE allowed retrieving AOT over lesser areas than the previous codes but with significantly higher levels of confidence. For this study, the overall improvement in AOT mapping in terms of the area over which AOT was reliably retrieved was estimated to 27%. The correlation between satellite retrieved AOT values and limited ground based data was satisfactory during this preliminary assessment. CHRISTINE also returned a rough approximation of the dominant aerosol size distribution categories on the basis of Ångstrom exponent calculation. Future work will address an extended validation of these results over other urban sites.

The new code also overcame speed calculation constraints, which were a limiting factor for the previous codes. A remaining limitation is that the code is still depended on contrast reduction therefore its application is restricted to highly contrasted areas, favoring the application of the method over urban sites. Accordingly CHRISTINE is not appropriate for homogeneous areas such as extended agricultural, forested, desert or snowed regions. Another inherent limitation of the satellite data used by the code is the infrequent overpasses of high spatial resolution. The use of satellite data acquired by sensors with daily overpasses, such as MODIS or MERIS, would, however, enable AOT retrieval on a daily basis for the assessment of short-term exposure to pollutants.

These preliminary results show that the new code can be applied to high resolution satellite data to improve air quality monitoring in urban areas by supplementing the spatial nature of the existing urban monitoring networks. Detailed space resolved estimates on air pollution over urban areas by satellite can be useful towards complying with the European air quality Framework Directive 96/62/EC, and also lead to improvements in air quality monitoring networks deployment. In the case of Athens the application of the code to archived satellite data also allowed hindcasts for the period prior to ground based particulate measurements.

#### References

- Borowiak, A., Dentener, F. (Eds.), 2006. Institute for Environment and Sustainability, Directorate-General Joint Research Centre, European Commission, EUR 22330 EN.

- Chu, D.A., Kaufman, Y.J., Zibordi, G., Chern, J.D., Jietai, M., Chengcai, L., Holben, B.N., 2003. Global monitoring of air pollution over land from the Earth Observing System-Terra Moderate Resolution Imaging Spectroradiometer (MODIS). *Journal of Geophysical Research* 108, 4661.
- Colls, J., 1997. *Air Pollution: An Introduction*. E & FN Spon Publisher, London 341 p.
- Cvitas, T., Guesten, H., Heinrich, G., Klasinc, L., Lalas, D.P., Petrakis, M., 1985. Characteristics of air pollution during the summer in Athens, Greece. *Staubtechnik—Reinhalung der Luft* 45, 297.
- Dandou, A., Bossioli, E., Tombrou, M., Sifakis, N., Paronis, D., Soulakellis, N., Sarigiannis, D., 2002. The importance of mixing height in characterising pollution levels from aerosol optical thickness derived by satellite. *Water, Air, and Soil Pollution: Focus* 2, 17–28.
- Eikvil, L., Aurdal, L., Koren, H., 2009. Classification-based vehicle detection in high-resolution satellite images. *ISPRS Journal of Photogrammetry and Remote Sensing* 64, 65–72.
- Engel-Cox, J., Hoff, R.M., Haymet, A.D.J., 2004. Recommendations on the use of satellite remote-sensing data for urban air quality. *Journal of the Air & Waste Management Association* 54 (11), 1360–1371.
- Fraser, R.S., Gaut, N.E., Reifstein, E.C., Sievering, H., 1983. Interaction mechanisms within the atmosphere. In: Reeves, R.G. (Ed.), *Manual of Remote Sensing, Manual of Remote Sensing*, I, R. G. Reeves, Ed., Chapter 5, 207–210, American Society of Photogrammetry, Falls Church, Virginia.
- Fraser, R.S., Kaufman, Y.J., Mahoney, R.L., 1984. Satellite measurements of aerosol mass and transport. *Atmospheric Environment* 18, 2577–2584.
- Gordon, H.R., Clark, D.K., 1981. Clear water radiances for atmospheric correction of Measurements of atmospheric optical thickness over water using ERTS-1 data. *Applied Optics* 20, 4175–4180.
- Griggs, M., 1975. Measurement of atmospheric optical thickness over water using ERTS-1 data. *Journal of the Air Pollution Control Association* 25, 622–626.
- Gupta, P., Christopher, S.A., Wang, J., Gehrig, R., Lee, Y., Kumar, N., 2006. Satellite remote sensing of particulate matter and air quality assessment over global cities. *Atmospheric Environment* 40, 5880–5892.
- Hsu, N.C., Tsay, S.C., King, M.D., Herman, J.R., 2004. Aerosol properties over bright-reflecting source regions. *IEEE Transactions on Geoscience and Remote Sensing* 42 (3), 557–569.
- Jiang, X., Liu, Y., Ming Jiang, B.W., 2007. Comparison of MISR aerosol optical thickness with AERONET measurements in Beijing metropolitan area. *Remote Sensing of Environment* 107, 45–53.
- Kambezidis, H.D., Tulleken, R., Amanatidis, G.T., Paliatsos, A.G., Asimakopoulos, D.N., 1995. Statistical evaluation of selected air pollutants in Athens, Greece. *Environmental Science and Technology* 29, 349–361.
- Kambezidis, H.D., Weidauer, D., Melas, D., Ulbrich, M., 1998. Air quality in the Athens basin during sea breeze and non sea breeze days using laser-remote-sensing technique. *Atmospheric Environment* 32 (12), 2173–2182.
- Kambezidis, H., Sifakis, N., 2004. Air quality in the greater Athens area. Contribution to: Urban Air Pollution. In: Klumpp, A., Ansel, W., Klumpp, G. (Eds.), *Bioindication and Environmental Awareness, Chapter 1: Bioindication and Environmental Monitoring*, Cuvillier Verlag, Göttingen.
- Kaskaoutis, D.G., Kambezidis, H.D., Adamopoulos, A.D., Kassomenos, P.A., 2006a. Comparison between experimental data and modeling estimates of aerosol optical depth over Athens, Greece. *Journal of Atmospheric and Solar-Terrestrial Physics* 68, 1167–1178.
- Kaskaoutis, D.G., Kambezidis, H.D., Adamopoulos, A.D., Kassomenos, P.A., 2006b. On the characterization of aerosols using the Ångström exponent in the Athens area. *Journal of Atmospheric and Solar-Terrestrial Physics* 68, 2147–2163.
- Kaufman, Y.J., Sendra, C., 1988. Algorithm for atmospheric corrections. *International Journal of Remote Sensing* 9, 1357–1381.
- Kocifaj, M., Horvath, H., 2005. Retrieval of size distribution for urban aerosols using multispectral optical data. *Journal of Physics: Conference Series* 6, 97–102.
- Kokhanovsky, A.A., Breon, F.M., Cacciari, A., Carboni, E., Diner, D., Di Nicolantonio, W., Grainger, R.G., Grey, W.M.F., Höller, R., Lee, K.H., Li, Z., North, P.R.J., Sayer, A.M., Thomas, G.E., von Hoyningen-Huene, W., 2007. Aerosol remote sensing over land: a comparison of satellite retrievals using different algorithms and instruments. *Atmospheric Research* 85, 372–394.
- Lalas, D.P., Asimakopoulos, D.N., Deligiorgi, D.G., Helmis, C., 1983. Sea-breeze circulation and photochemical pollution in Athens. *Atmospheric Environment* 17, 1621–1632.
- Lenoble, J., 1993. *Atmospheric Radiative Transfer*. Deepak Publishing, Hampton, VA.
- Liang, S., Zhong, B., Fang, H., 2006. Improved estimation of aerosol optical depth from MODIS imagery over land surfaces. *Remote Sensing of Environment* 104 (4), 416–425. References and further reading may be available for this article.
- Liu, Y., Franklin, M., Kahn, R., Koutrakis, P., 2007. Using aerosol optical thickness to predict ground-level PM<sub>2.5</sub> concentrations in the St. Louis area: a comparison between MISR and MODIS. *Remote Sensing of Environment* 107, 33–44.
- Marey, H., Gille, J., El-Askary, H., Shalaby, S., El-Raey, M., 2010. Study of the formation of the “Black Cloud” and its dynamics over Cairo, Egypt using MODIS and MISR sensors. *Journal of Geophysical Research* 115, D21206.
- Middleton, W.E.K., 1952. *Vision Through the Atmosphere*. University of Toronto Press, Toronto.
- Nichol, J.E., Wong, M.S., 2009. High resolution remote sensing of densely urbanised regions: a case study of Hong Kong. *Sensors* 9, 4695–4708.
- Popp, C., Hauser, A., Foppa, N., Wunderle, S., 2007. Remote sensing of aerosol optical depth over central Europe from MSG-SEVIRI data and accuracy assessment with ground-based AERONET measurements. *Journal of Geophysical Research* 112, D24S11.
- Potter, J.F., Medlowitz, M.A., 1975. On the determination of Haze Levels from Landsat Data. In: *Proceedings of the 10th International Symposium on Remote Sensing of the Environment*, Ann Arbor, 695–703.
- Retalis, A., Sifakis, N., 2010. Urban aerosol mapping over Athens using the differential textural analysis (DTA) algorithm on MERIS-ENVISAT data. *ISPRS Journal of Photogrammetry and Remote Sensing* 54, 17–25.
- Sarigiannis, D., Soulakellis, N., Sifakis, N., 2004. Information fusion for computational assessment of air quality and health effects. *Photogrammetric Engineering and Remote Sensing* 70, 235–245.
- Schaefer, K., Harbusch, A., Emeis, S., Koepke, P., Wiegner, M., 2008. Correlation of aerosol mass near the ground with aerosol optical depth during two seasons in Munich. *Atmospheric Environment* 42, 4036–4046.
- Scheff, P.A., Valiozis, C., 1990. Characterization and source identification of respirable particulate matter in Athens, Greece. *Atmospheric Environment* 24A, 203–211.
- Sifakis, N., 1987. *Tentative Mapping of Air Pollution Using SPOT Satellite Images (M.S. thesis (DESS))*. University Paris-6, doc: GDTA-Toulouse, ENSG-Paris, CNES-Toulouse, 30 p.
- Sifakis, N., Deschamps, P.Y., 1992. Mapping of air pollution using spot satellite data. *Photogrammetric Engineering and Remote Sensing* 58, 1433–1437.
- Short, N.M., Lowman Jr., P.D., Freden, S.C., Finch Jr., W.A., 1976. *Mission to Earth: Landsat Views of the World*. NASA, Scientific and Technical Information Office, Washington D.C. p. 459.
- Tang, J., Xue, Y., Yu, T., Guan, Y.N., 2005. Aerosol optical thickness determination by exploiting the synergy of TERRA and AQUA MODIS. *Remote Sensing of Environment* 94, 327–334.
- Tanré, D., Deschamps, P.Y., Devaux, C., Herman, M., 1988. Estimation of Saharan aerosol optical thickness from blurring effects in Thematic Mapper data. *Journal of Geophysical Research* 93, 15955–15964.
- Von Hoyningen-Huene, W., Freitag, M., Burrows, J.B., 2003. Retrieval of aerosol optical thickness over land surfaces from top-of-atmosphere radiance. *Journal of Geophysical Research* 108 (D9), 4260.